



ARTICLE

A Solvation Model for Performance Enhancement of Dye-Sensitized Solar Cells

Adel Daoud^{1,2,3,4,*}, Ali Cheknane², Jean Michel Nunzi^{3,4} and Afak Meftah¹

¹Laboratoire des Matériaux Semi-Conducteurs et Métalliques (LMSM), Université de Biskra, Biskra, Algeria

²Laboratoire des Semi-Conducteurs et Matériaux Fonctionnels (LSMF), Université Amar Telidji de Laghouat, Laghouat, Algérie

³Department of Chemistry, Queen's University, Kingston, Canada

⁴Department of Engineering Physics and Astronomy, Queen's University, Kingston, Canada

*Corresponding Author: Adel Daoud. Email: adel.daoud@univ-biskra.dz; daoudadel13@gmail.com

Received: 20 February 2022 Accepted: 28 April 2022

ABSTRACT

A solubility model for Merocyanine-540 dye together with the interface's electron transfer kinetics of MC-540/TiO₂ has been investigated (Merocyanine 540-based dye has been used effectively in dye-sensitized solar cells). The highest absorption peaks were recorded at 489 nm and 493 nm in Water and Ethanol solvent, vs. the vacuum phase which yielded 495 nm (associated with a modest electron injection-free energy value (ΔG_{inj}) of -2.34 eV for both Water and Ethanol solvents). The time-dependent density functional theory (TD-DFT) method approach has been applied in this simulation. Additionally, the electronic structure and simulated UV-Vis spectra of the dye in different solvents have been determined, and the alignment with the solar spectrum has been discussed to a certain extent. The energy level diagrams and electron density of the primary molecular orbitals are shown, and the major issues that have an impact on our new interface's performance are examined. It is concluded that the proposed Solvation Model (SM) can improve the performance of Dye-Sensitized Solar Cells.

KEYWORDS

Mc-540-based dye; DFT method; electron injection; n-DSSCs

1 Introduction

Since Grätzel et al. published the prototype of the dye-sensitized solar cell (DSSC) in 1991 [1,2], it has sparked intense interest over the last decades due to the low cost and simple preparation process. In addition to developing many dyes to maximize efficiency, many attempts have been made to boost the performance of DSCs, such as replacing titania film electrodes (TiO₂) with other semiconductors [3], or adopting many less negative mediators, such as cobalt [4], in addition to developing many dyes to maximize efficiency.

Generally, in DSC, some requirements should be satisfied, like broad optical absorption and avoiding dye aggregation. E_{HOMO} and E_{LUMO} levels of the dye used must be compatible with the energy level of the semiconductor edge and redox couples to allow effective light-harvesting efficiency (LHE) and reduce the charge recombination (CR) at the semiconductor-electrolyte interface [5]. To provide adequate driving force at least 0.2 eV for electron injection with the sensitizer's LUMO must be higher (more negative) than TiO₂'s conduction-band edge (CBE) (-0.5 V vs. NHE) [5]. For successful dye regeneration, the dye HOMO ought to be more positive at least 0.15 eV than the redox energy level [6]. For the dye to bond



with the semiconductor surface, it must have suitable anchoring groups, such as carboxylates or phosphonates [7]. This is needed to make the shift of the electrons of the excited dye to the semiconductor.

Various sensitizers have already been investigated for n-type DSSC devices, as well as metal-free organic dyes, metal complexes, phthalocyanines, porphyrins, etc. [8]. N3 and N719 dyes are amongst the best sensitizers employed in n-DSCs and are commonly utilized as reference dyes [9]. These include various dyes based on metal complexes, the N719 dye has a high performance [8]. Ru(II)-polypyridyl complexes have been stated to have an n-value of 12% or more [4]. There are several options for improving production, as well as a sustainable and affordable renewable energy source.

Numerous papers have shown that the DFT methods can be used to analyze the electronic and optical properties of DSCs devices, which are widely employed, such as Gaussian09, Quantum Espresso [10], ADF [11], and Material Studio software (Dmol3 code) [12]. In this paper, we investigate the effect of the solvation model on both injection electron and dye regeneration rates, using Material Studio software in the first principal computational analysis. GGA functional is used to measure the electronic and optical properties after dye optimization.

2 Computational Details

The calculations were done using the DFT method [13–16], with a three-dimensional periodic crystal and the optimization step in Dmol3 code. The GGA functional is known to be effective in reliably predicting structural transition pressures [17]. It operates in more complex structures, whereas in Dmol3 code, including the solvation model with no symmetry constraints. Materials Studio was created to reduce error in completely converged all-electron DFT calculations. Whereas, using quantum chemistry's basis sets and integral methods, simulation helps one to gain insight. Where the geometry optimization of the ground state of Mc-540 dye was performed in Water and Ethanol solvents and also in the Vacuum phase, in Dmol3 code which is including GGA functional [16,17], and DNP basis set was employed in geometry optimization [18]. The doubled numerical basis set (DNP, including polarization d-function) is chosen as the basis set, which is equivalent to the Gaussian 6–31G (d, p) basis set and has a higher accuracy set [19]. The simulation was carried out in Materials Studio 2016 (MS) software [20]. The Electronic and Optical properties of Mc-540 dye were performed out in the same functional and basis set (GGA-DNP) is presented in Table 1.

Table 1: Other input parameters

Parameters calculation	Functional	Basis set	Task energy	Energy	Max force	Max displacement
Geometry optimization	GGA	DNP	Customized quality	1.0×10^{-6} Ha	4.0×10^{-4} Ha/Å	5.0×10^{-4} Å
Electronic properties	GGA	DNP	Customized quality	/	/	/
Optical properties	GGA	PBE	Customized quality	/	/	/

3 Results and Discussion

3.1 Structure of Merocyanine-540 Dye

Merocyanines are a kind of polymethine dyes [21–23] with well-defined structural characteristics. Merocyanines are part of a class of dyes known as functional dyes [24], which have uses that are dictated not just by their color but also by their useful chemical characteristics. Typically, these dyes are brightly colored and have high extinction coefficients. Merocyanine-540 dye was used in many applications, for example, it was used in biological membranes applications [25], and live cells [26]. Its structure is shown in Fig. 1.

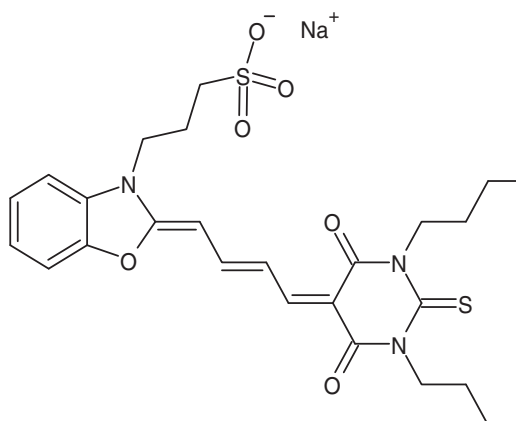


Figure 1: The molecular structure of the merocyanine-540 dye

3.2 Alignment of Energy Levels and Electron Transfer

To study the feasibility of charge injection into the semiconductor and dye regeneration, we used DFT simulations to determine the energy level alignment of the dye with the substrate and the electrolyte by calculating the energies of the dye's ground and excited states and the energy of the conduction band edge (CBE) for non-interacting TiO_2 electrode, as well as the redox level of the $(\text{I}^-/\text{I}_3^-)$ electrolyte (see Section 4.3 below). The singlet-to-singlet transitions between the deprotonated MC-540 dye in different solvents are shown by the transition arrow. Fig. 2 shows the values on the axes vs. the vacuum.

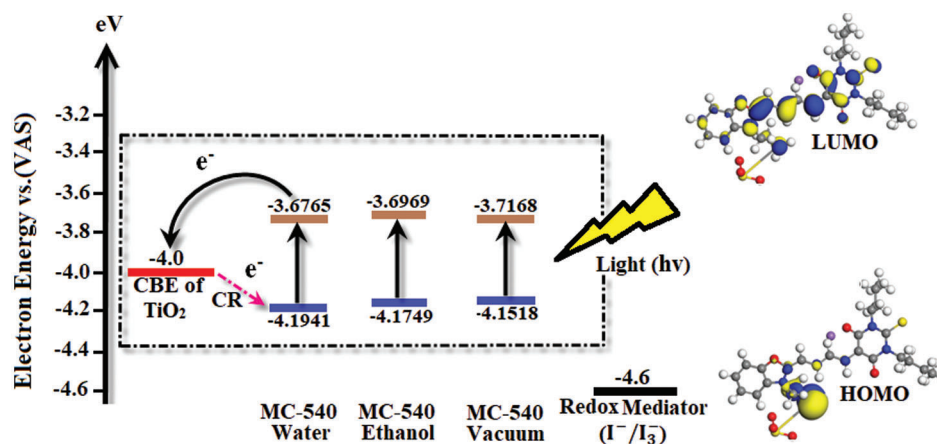


Figure 2: The schematic energy diagram of the merocyanine-540 dye in water, ethanol solvents, vs. the vacuum phase, together with the non-interacting TiO_2 semiconductor and redox mediator $(\text{I}^-/\text{I}_3^-)$

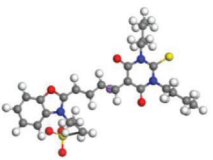
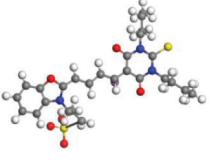
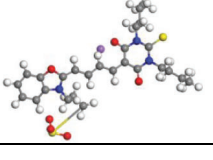
The energy levels vary and can adsorb to the TiO_2 surface. Where, the LUMO's levels in the three cases are higher than the TiO_2 CBE, allowing for easier electron injection into the semiconductor. Moreover, the HOMO level energies are changed in each solvent, which needs more experimental research on our new interface of MC-540@ TiO_2 DSCs.

3.3 Electronic Properties of Merocyanine-540 Dye

Generally, the suitable Donor and Acceptor groups are improving the DSSC LHE value. The powerful Donor group exhibits a higher HOMO energy level (E_{HOMO}), while the strong group Acceptor exhibits a lower LUMO energy level (E_{LUMO}). We calculated the boundary molecular orbitals, which represent the difference energy between HOMO and LUMO of Mc-540 dye, as shown in Table 2 below. Where the energy

gap values for Water and Ethanol are 0.5175 and 0.4779 eV, respectively, vs. 0.4350 eV for the vacuum phase. Notably, the value of E_g in the Ethanol solvent is narrower than in the Water solvent is due to the increased transfer of charge from the Donor unit to the Acceptor unit in the Ethanol compared to the Water.

Table 2: Electronic properties for merocyanine-540 dye are calculated using the GGA-DNP function in water, ethanol solvent, and vacuum phase

Solvents	Optimized Geometry	HOMO eV	LUMO eV	H-L eV
Water		-4.1941	-3.6765	0.5175
Ethanol		-4.1749	-3.6969	0.4779
Vacuum		-4.1518	-3.7168	0.4350

We offered the densities of state (DOS) of MC-540 dye in different solvents by using the GGA functional and plotted in Fig. 3 above, which is changed in several phases, which indicates that the effect of the solvation model on Dye-Sensitized Solar Cell (DSC). The energies of LUMO and HOMO changed slightly in three phases, which resulted in a noticeable change in electron injection efficiency.

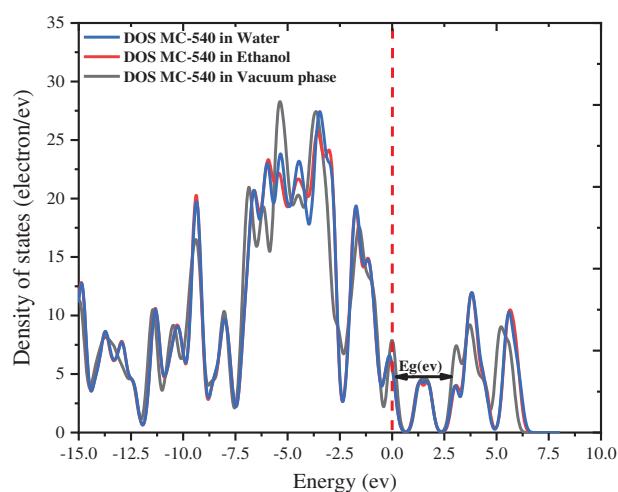


Figure 3: The densities of state (DOS) of merocyanine-540 dye in water, ethanol solvent, and vacuum phase

Different solvents exhibit different energy levels of HOMO and LUMO. This means that the relationship between the acceptor and donor is affected by the energy levels, which consequently change the driving force. Where resulted in modest injection rates of -2.3408 , -2.3400 , and -2.3531 eV, respectively for the

Water, Ethanol, and Vacuum phase. Electronic transitions have been calculated for all the studied solvents to better understand their excited states (as rigorously described in the next section). Our simulation shows that the electronic properties can be controlled through the solvation model, this is also demonstrated by changing the red-shift range of the optical properties of the MC-540 dye as presented in Fig. 4 below. As a result, the choice of the appropriate solvent is attributed to improving the microscopic properties (ΔG_{inj}), (ΔG_{reg}). In addition, the electronic transition, HOMO to LUMO, in the visible domain is the most intense and is closely related to the ICT from donor units to acceptors anchoring groups across a conjugated bridge, this transition corresponds to HOMO to LUMO excitation, with the HOMO being mostly located near to the anchoring group (SO_3 group) that possesses a donor character, whereas the LUMO is almost entirely found on the more accepting moiety for all the solvents.

3.4 Absorption Spectrum

Time-dependent density functional theory (TD-DFT) calculations are still one of the most common methods for evaluating the absorption properties of dye molecules due to their accuracy and low computational cost. It is undeniable that careful selection of the exchange/correlation (XC) function is important for accurately describing the absorption spectrum of MC-540 dye used in DSCs with non-negligible charge transfer (CT) properties [27]. Unfortunately, the TD-DFT method is not used to calculate the UV-Vis absorption spectra because it is not supported by the B3LYP XC in the Demol3 code Fig. 4.

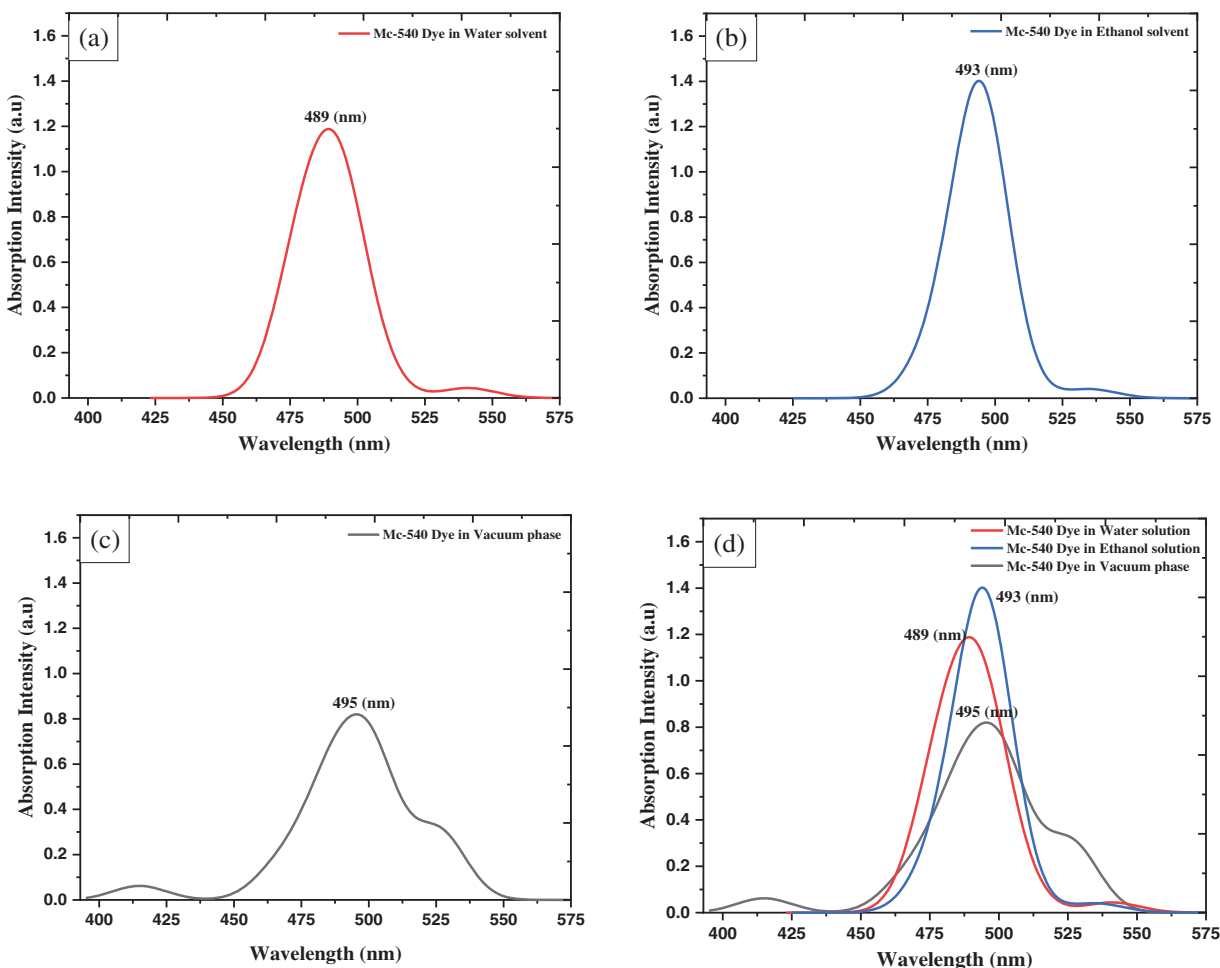


Figure 4: The UV/Vis absorption spectra of merocyanine-540 dye in the water, ethanol solvent, and vacuum phase using GGA-PBE XC functional

The ability of a sensitizer to cover the visible region 400 to 800 nm and its proximity to the infrared region (IR) is a very important feature. Fortunately, the main absorption peaks, for MC-540 dye, are in the visible area, which is from (400 to 575 nm). The absorption peaks match the π - π^* intra-molecular transitions, this suits an effective charge separation. As far as we know, MC-540 dye was not reported as a photosensitizer in DSCs before. From the literature, the MC-540 dye was employed on a Sensor System (SS) [28] and tested for Hybrid Solar Cell (HSC) applications, in which it aggregated on the ZnS and CdS surfaces [29]. Where in this work they found an absorption maximum at 565 nm.

Calculations show that MC-540 dye would be a good photosensitizer in DSCs. Where the present simulation shows that the MC-540 dye has a peak at 489 nm corresponding to an oscillator strength (f) of 1.188399 in Water solvent, and (493 nm, 1.402295) in the Ethanol solvent, Table 3. Our results indicate that the Ethanol solvent expands the light absorption range compared to the Water solvent. Therefore, it is expected that the performance of the soluble dye in Ethanol will outperform the Water-soluble dye. The photo-physical properties rely on the (D- π -A) design, where the MC-540 dye has been changed in different solvents. The reason for poor DSSC performance is electrical and optical loss. Therefore, as Snaith suggested, reducing light loss can improve performance. In particular, the optical loss and large potential loss due to the conversion of absorbed photons into the optical bandgap of the dye and the V_{OC} generated across the solar cell are emphasized. The potential loss of DSSC with current state-of-the-art technology (0.75 eV) and value absorption of λ at 840 nm, so a maximum PCE of 13.4% could be obtained [30]. This can be applied to MC-540 dye here by the solvation model, where the appropriate solvent would lead to enhancing the optical and physical properties. Additionally, the molecular modifications at the level of the dye also would raise the light-harvesting efficiency (LHE) and thus reduce the losses, which we have mentioned above. Finally, we improved the properties optical of the sensitizer that affected the driving force of electron transmission. This is evidenced by the calculated electrochemical properties in the next section, as a result of this simulation, the solvation model will affect the overall performance of the DSCs based on MC-540 dye.

Table 3: Optical properties of MC-540 dye calculated by using GGA-PBE, in water and ethanol solvent, vs. vacuum phase, compared with experimental data, Hybrid Solar Cell (HSC) [29], Sensor System (SS) [28]

Optical properties	Solvent	Absorption λ (DSC)		Absorption λ_1 (HSC)		Absorption λ_2 (SS)
Computational results	Unit	nm	eV	nm	nm	nm
	Water	489	2.535	565	563 (Mc-540/ZnS)	560
	Ethanol	493	2.515	565	560 (Mc-540/CdS)	/
	Vacuum	495	2.505	/	/	/

4 Electronic Parameters Influencing PCE

4.1 The Short Circuit Photocurrent Density (J_{SC}) and the Light-Harvesting Efficiency (LHE)

As shown in Eq. (1), the short-circuit photocurrent density (J_{sc}) consists of various parameters. Where the J_{sc} has an essential association with LHE and the Oscillator Strength (f) at λ_{max} which has a major impact on the absorption spectra and thus also affects the photon current Efficiency (PCE), LHE is calculated using Eq. (2) [27]. A high value for Φ_{inj} might enhance the J_{sc} (See Eq. (1)) which is neatly related to the driving force of the electron injection from the photo-induced excited states of the dye to the TiO_2 electrode. The following is the order of MC-540 dye based on LHE matching: LHE (Ethanol) > LHE (Water) > LHE (Vacuum), As illustrated in Fig. 5b.

$$J_{sc} = \int_{\lambda}^0 LHE(\lambda)_{inj} n_{collect} d\lambda \quad (1)$$

$$LHE = 1 - 10^{-f} \quad (2)$$

The LHEs values of Mc-540 dye in the Water, Ethanol solvent and Vacuum phase are 0.9351, 0.9603, and 0.8487, respectively. Where in the Ethanol solvent the LHE is larger than Water, due to the largest oscillator strength (f) in Ethanol. Moreover, the electron injection rate can be improved based on optimizing the LHE. Where the LHE photocurrent response correlates with a high LHE (λ). So it should come as no surprise that LHE is a suitable standard for enhancing DSCs devices through appropriate solutions to ensure the highest harvesting efficiency (LHE). Additionally, it ensures the highest dye loading on the semiconductor surface through the expected strong adsorption on the electrode surface. Where Fig. 5a shows the measured (LHE) vs. absorption wavelengths (λ) for MC-540 dye in different solvents. Dye molecules MC-540 in all cases have strong light harvesting potential in the visible spectrum, with LHE (λ) values close to 100%, whereas MC-540 in the Ethanol solution has a broader coverage compared to the Water solution. This indicates that elongating the conjugated bridges of the dye molecules inevitably lead to a decrease in H-L, expanding the absorption band, and enhancing light-harvesting abilities.

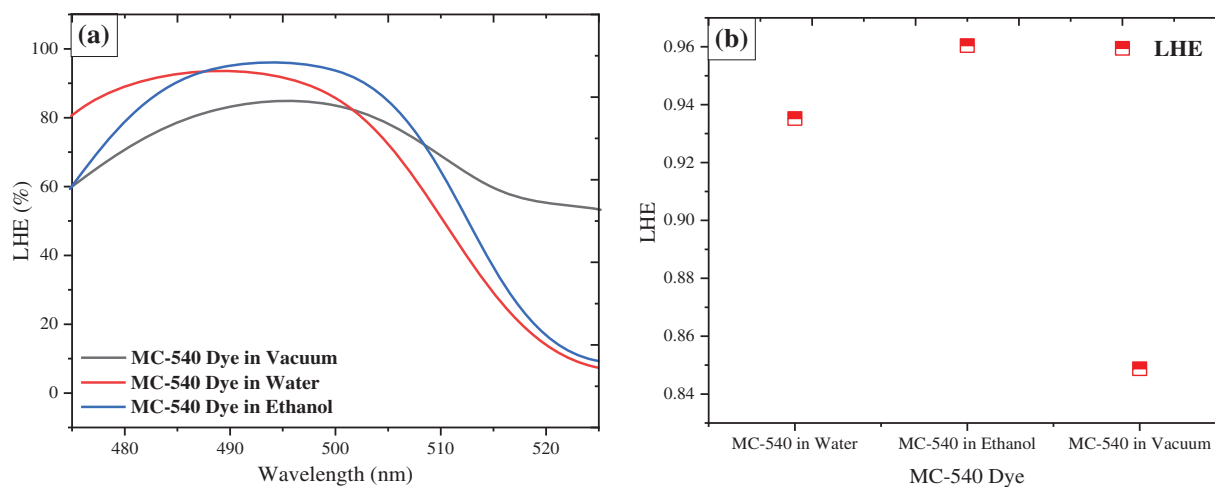


Figure 5: The light harvesting efficiency (LHE) spectra of the Mc-540 dye in the water, ethanol solvent, and vacuum phase

4.2 The Open Circuit Potential

According to the relationship between V_{OC} and E_{LUMO} of the dye, we can express the V_{oc} of the Mc-540/TiO₂ interface in different solvents. Where the E_{LUMO} is the LUMO of the dye. While the E_{CB} is the conduction-band edge of the TiO₂ electrode, the V_{oc} can be expressed by Eq. (3) [31–33]. Our study indicates that the values of V_{oc} of the dye in various solutions calculated using Eq. (3), the values took range from 0.5531 to 0.5934 eV (Table 4). The Water increased the stress in the open circuit by 0.5934 eV which is more than the Ethanol and the Vacuum phase of 0.5730 and 0.5531 eV, respectively.

$$VOC = ELUMO - ECB \quad (3)$$

Table 4: Approximated electrochemical parameters of the Mc-540 dye in the water and ethanol solvents, vs. the vacuum phase

Parameters calculation	Solvent	E_{Dye}^{ox}	E_{Dye*}^{ox}	ΔG_{inj}	ΔG_{reg}	LHE	Voc
Computational results	Unit	eV	eV	eV	eV	/	eV
	Water	-4.1941	-1.6591	-2.3408	0.4058	0.9351	0.5934
	Ethanol	-4.1750	-1.6591	-2.3400	0.4250	0.9604	0.5730
	Vacuum	-4.1519	-1.6469	-2.3531	0.4481	0.8487	0.5531

4.3 Quantum Chemical Calculations

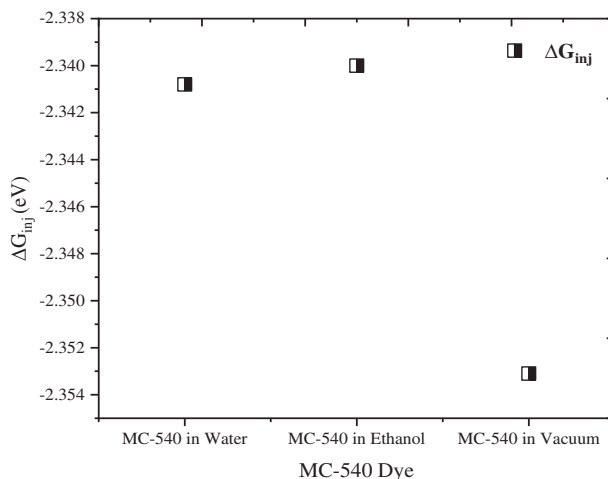
The ground state oxidation potential E_{Dye}^{ox} and the excited state oxidation potential E_{Dye*}^{ox} of the sensitizer are important parameters to determine the Electrochemical Properties for DSC such as the driving force of electron injection (ΔG_{inj}) and dye regeneration (ΔG_{reg}). They were illustrated and measured in Table 4 and Fig. 6. The E_{Dye}^{ox} is regarded as the HOMO energy of the sensitizer, according to Koopmans's theorem, the E_{Dye*}^{ox} , the formulas in the following Eqs. (4)–(6) [27,34,35] are used to compute ΔG_{inj} , and ΔG_{reg} , respectively.

$$\Delta G_{inj} = [E_{Dye*}^{ox} - E_{TiO_2}^{CBE}] \quad (4)$$

$$\Delta G_{reg} = [E_{I^-/I_3^-}^{ox} - E_{Dye}^{ox}] \quad (5)$$

$$E_{Dye*}^{ox} = [E_{Dye}^{ox} - \lambda_{max}^{ICT}] \quad (6)$$

where λ_{max}^{ICT} is the maximum absorption energy of the dye and E_{CB} is the reduction potential of the conduction band of semiconductor TiO_2 (-4.0) eV [27], and the redox potential $E_{I^-/I_3^-}^{ox}$ is taken as -4.6 eV [27] and the E_{Dye*}^{ox} can be estimated by the difference energy between the oxidation potential energy of the dye E_{Dye}^{ox} and the maximum absorption energy λ_{max}^{ICT} . The negative ΔG_{inj} refers to the electron injection as a spontaneous process [36,37]. The sequence of dye regeneration for various solvents is as follows: MC-540 (Vacuum) > MC-540 (Water) > MC-540 (Ethanol), Table 4, as a result, the dye regeneration in all the solvents is not enough. Where the dye regeneration process (ΔG_{reg}) is difficult due to the dye's molecular level (E_{HOMO}) is not aligned with the energy level of the electrolyte pairs (I^-/I_3^-). However, we expect a high recombination reaction in which resulting from the convergence of the semiconductor conduction band edge TiO_2 , and the LUMO energy level of the dye may lead to reduced overall performance in DSCs based on an MC-540/ TiO_2 interface.

**Figure 6:** The free energy values of the electron injection at the MC-540/ TiO_2 interface in the water, ethanol solvent, and vacuum phase

A more negative value would provide a larger driving force [35]. The Quantum chemical calculations indicate that the dye regeneration process (ΔG_{reg}) allows us to observe a slight deviation, where the Mc-540 dye regeneration values are different, and the electron injection process (ΔG_{inj}) is convergent in all solvents, which has a value of -2.34 eV in both solvents as seen in Fig. 6.

The LHE in Ethanol solvent yielded a value of 0.9604 compared to Water which gave a value of 0.9351 vs. the Vacuum phase 0.8487 due to enhancement in the electronic properties. Meanwhile, the Water solvent increases the open circuit V_{OC} of 0.5934 eV compared to the Ethanol solvent which has recorded a value of 0.5730 eV due to the viscosity which is changed in each solvent [38].

5 Conclusion

Finally, we have presented a new interface based on Merocyanine-540 dye as a photo-sensitizer for Dye-Sensitized Solar Cells applications. Using the first computational analysis of the MC-540 dye in the Water, Ethanol solvent, and Vacuum phase. The calculations were carried out using the DFT method. Where, the GGA functional was used for electronic and optical properties, and the DNP (including polarization d-function) basis set was chosen because it is equivalent to the Gaussian09 6-31G (d, p) basis set and has high precision compared to other basis sets for the electronic properties. While the PBE basis Set was employed for optic properties. Additionally, we determined the Electrochemical properties by simulation, instead of the costlier cyclic voltammetry. Our simulation indicates that the Mc-540 dye's band gap energies changed in several phases, which proves the solvation model's effect on Dye-Sensitized Solar Cells (DSSCs). In three phases, the LUMOs and HOMOs energies of the dye have changed slightly, which affected the electron injection and dye regeneration efficiency. In both solvents, the electron injection rate was equal to -2.34 eV. The water solvent reduced the interface barrier by reducing the HOMO level to become more negative as the free energy of dye regeneration (ΔG_{reg}) decreased from 0.4250 to 0.40582 eV, vs. the Vacuum phase, which has a rate of 0.4481 eV. Our simulation shows that DSC with various solutions can be improved the Light-Harvesting Efficiency (LHE). Where the light harvest was superior in the Ethanol solution than the Water solution. This indicates that it is possible to invest in the Mc-540 dye, but with conditions. However, it suffers from the problem of dye regeneration and fast recombination reaction between the LUMO of the dye and the conduction band edge (CBE) of the TiO_2 semiconductor. Where the dye regeneration mechanism (ΔG_{reg}) is complicated because the dye's molecular level (E_{HOMO}) is not matched with the energy level of the electrolyte pairs (I^-/I_3^-), which may limit the overall performance of the device. This problem can be solved by using a more negative electrolyte than (I^-/I_3^-), such as cobalt. All calculations were performed using BIOVIA's Materials Studio 2016 (MS) software.

Author Statement: All co-authors have made significant contributions to this work and deserve to be listed as co-authors.

Funding Statement: Financial support for this work by the Natural Sciences and Engineering Research Council of Canada (NSERC), Grant No. RGPIN-2020-07016, Canada's Federal Funding Agency for University-Based Research and Student Training is acknowledged.

Conflicts of Interest: There are no known competing financial interests or personal relationships that could have influenced the work described in this document paper.

References

1. Grätzel, M., O'Regan, B. (1991). A low-cost, high-efficiency solar cell based on dye-sensitized colloidal TiO_2 films. *Nature*, 353(6346), 737–740. DOI 10.1038/353737a0.
2. Daoud, A., Cheknane, A., Meftah, A., Michel, J. N., Shalabi, M. et al. (2022). Spatial separation strategies to control charge recombination and dye regeneration in p-type dye sensitized solar cells. *Solar Energy*, 236, 107–152. DOI 10.1016/j.solener.2022.02.050.

3. Habibi, M. H., Mikhak, M., Zendehdel, M., Habibi, M. (2012). Influence of nanostructured zinc titanate, zinc oxide or titanium dioxide thin film coated on fluorine doped Tin oxide as working electrodes for dye-sensitized solar cell. *International Journal of Electrochemical Science*, 7(8), 6787–6798.
4. Yella, A., Lee, H. W., Tsao, H. N., Yi, C., Chandiran, A. K. et al. (2011). Porphyrin-sensitized solar cells with cobalt (II/III)-Based redox electrolyte exceed 12 percent efficiency. *Science*, 334(6056), 629–634. DOI 10.1126/science.1209688.
5. Hara, K., Sato, T., Katoh, R., Furube, A., Ohga, Y. et al. (2003). Molecular design of coumarin dyes for efficient dye-sensitized solar cells. *The Journal of Physical Chemistry B*, 107(2), 597–606. DOI 10.1021/jp026963x.
6. Wenger, S., Bouit, P. A., Chen, Q., Teuscher, J., di Censo, D. et al. (2010). Efficient electron transfer and sensitizer regeneration in stable π -extended tetrathiafulvalene-sensitized solar cells. *Journal of the American Chemical Society*, 132(14), 5164–5169. DOI 10.1021/ja909291h.
7. Yum, J. H., Baranoff, E., Wenger, S., Nazeeruddin, M. K., Grätzel, M. (2011). Panchromatic engineering for dye-sensitized solar cells. *Energy & Environmental Science*, 4(3), 842–857. DOI 10.1039/c0ee00536c.
8. Hagfeldt, A., Boschloo, G., Sun, L., Kloo, L., Pettersson, H. (2010). Dye-sensitized solar cells. *Chemical Reviews*, 110(11), 6595–6663. DOI 10.1021/cr900356p.
9. Jahantigh, F., Ghorashi, S. M. B., Bayat, A. (2020). Hybrid dye sensitized solar cell based on single layer graphene quantum dots. *Dyes and Pigments*, 175, 108118. DOI 10.1016/j.dyepig.2019.108118.
10. Shahzad, N., Risplendi, F., Pugliese, D., Bianco, S., Sacco, A. et al. (2013). Comparison of hemi-squaraine sensitized TiO₂ and ZnO photoanodes for DSSC applications. *The Journal of Physical Chemistry C*, 117(44), 22778–22783. DOI 10.1021/jp406824f.
11. Majid, A., Ullah, I., Kubra, K. T., Khan, S. U. D., Haider, S. (2019). First principles study of transition metals doped SiC for application as counter electrode in DSSC. *Surface Science*, 687, 41–47. DOI 10.1016/j.susc.2019.05.001.
12. Gada, E. A. M., Kamar, E. M., Mousa, M. A. (2020). Experimental and computational study on electronic and photovoltaic properties of chromen-2-one-based organic dyes used for dye-sensitized solar cells. *Egyptian Journal of Petroleum*, 29(2), 203–209. DOI 10.1016/j.ejpe.2020.04.002.
13. Calais, J. L. (1993). Density-functional theory of atoms and molecules. *International Journal of Quantum Chemistry*, 47(1), 101–101. DOI 10.1002/qua.560470107.
14. Hohenber, P., Kohn, W. (1964). Inhomogeneous electron gas. *Physical Review*, 136(3B), B864. DOI 10.1103/PhysRev.136.B864.
15. de Angelis, F., Fantacci, S., Selloni, A., Grätzel, M., Nazeeruddin, M. K. (2007). Influence of the sensitizer adsorption mode on the open-circuit potential of dye-sensitized solar cells. *Nano Letters*, 7(10), 3189–3195. DOI 10.1021/nl071835b.
16. De Angelis, F., Fantacci, S., Selloni, A. (2008). Alignment of the dye's molecular levels with the TiO₂ band edges in dye-sensitized solar cells: A DFT-TDDFT study. *Nanotechnology*, 19(42), 424002. DOI 10.1088/0957-4484/19/42/424002.
17. Jaffe, J. E., Snyder, J. A., Lin, Z., Hess, A. C. (2000). LDA and GGA calculations for high-pressure phase transitions in ZnO and MgO. *Physical Review B*, 62(3), 1660–1665. DOI 10.1103/PhysRevB.62.1660.
18. Abu-melha, S. (2018). Design, synthesis and DFT/DNP modeling study of new 2-Amino-5-arylazothiazole derivatives as potential antibacterial agents. *Molecules*, 23(434), 1–11. DOI 10.3390/molecules23020434.
19. Guo, M., Yang, H., Jian, X., Liang, J. L. Z., Han, P. et al. (2018). The adsorptions of fixed groups –CN, –NH₂, –SH, –OH and –COOH of dye molecules on stoichiometric, oxygen vacancy and Pt-doped SnO₂(110) surfaces. *Applied Surface Science*, 428(110), 851–860. DOI 10.1016/j.apsusc.2017.09.193.
20. Yu, S., Ahmadi, S., Zuleta, M., Tian, H., Schulte, K. et al. (2010). Adsorption geometry, molecular interaction, and charge transfer of triphenylamine-based dye on rutile TiO₂(110). *The Journal of Chemical Physics*, 133. DOI 10.1063/1.3509389.
21. Khazraji, A. C., Hotchandani, S., Das, S., Kamat, P. V. (1999). Controlling dye (Merocyanine-540) aggregation on nanostructured TiO₂ films. An organized assembly approach for enhancing the efficiency of photosensitization. *The Journal of Physical Chemistry B*, 103(22), 4693–4700. DOI 10.1021/jp9903110.

22. Zhang, Y., Görner, H. (2012). Photoprocesses of merocyanine 540 bound to serum albumin and lysozyme. *Journal of Molecular Structure*, 1011, 94–98. DOI 10.1016/j.molstruc.2011.07.042.
23. Gür, B., Meral, K. (2012). Preparation and characterization of mixed monolayers and langmuir-blodgett films of merocyanine 540/octadecylamine mixture. *Colloids and Surfaces A: Physicochemical and Engineering Aspects*, 414, 281–288. DOI 10.1016/j.colsurfa.2012.08.067.
24. Bürckstümmer, H. (2011). *Merocyanine dyes for solution-processed organic bulk-heterojunction solar cells (Ph.D. Thesis)*. Julius Maximilian University of Würzburg, Germany.
25. Smith, K. A., Conboy, J. C. (2011). Using micropatterned lipid bilayer arrays to measure the effect of membrane composition on merocyanine 540 binding. *Biochimica et Biophysica Acta (BBA)-Biomembranes*, 1808(6), 1611–1617. DOI 10.1016/j.bbamem.2011.02.017.
26. Chmyrov, V., Spielmann, T., Hevekerl, H., Widengren, J. (2015). *Trans-Cis* isomerization of lipophilic dyes probing membrane microviscosity in biological membranes and in live cells. *Analytical Chemistry*, 87(11), 5690–5697. DOI 10.1021/acs.analchem.5b00863.
27. Xu, Z., Li, Y., Zhang, W., Yuan, S., Hao, L. et al. (2019). DFT/TD-DFT study of novel T shaped phenothiazine-based organic dyes for dye-sensitized solar cells applications. *Spectrochimica Acta Part A: Molecular and Biomolecular Spectroscopy*, 212, 272–280. DOI 10.1016/j.saa.2019.01.002.
28. Bayraktutan, T., Gür, B., Demirbas, Ü. (2020). Detection of Al³⁺ and Fe³⁺ ions with phthalocyanine-merocyanine 540 Dye-based fluorescence resonance energy transfer. *Bulletin of the Korean Chemical Society*, 41(10), 973–980. DOI 10.1002/bkcs.12097.
29. Jabeen, U., Adhikari, T., Shah, S. M., Khan, S. U., Pathak, D. et al. (2018). Merocyanine-540 grafted on ZnS and CdS nanocrystals—An approach for enhancing the efficiency of inorganic- organic hybrid solar cell. *Optical Materials*, 83, 165–175. DOI 10.1016/j.optmat.2018.05.088.
30. Snaith, H. J. (2010). Estimating the maximum attainable efficiency in dye-sensitized solar cells. *Advanced Functional Materials*, 20(1), 13–19. DOI 10.1002/adfm.200901476.
31. Amkassou, A., Zgou, H. (2018). DFT and TD-DFT study of New D-II-A dyes for grätzel solar cell. *AIP Conference Proceedings*, 020003. DOI 10.1063/1.5084976.
32. Bourass, M., Benjelloun, A. T., Benzakour, M., Mcharfi, M., Hamidi, M. et al. (2016). The computational study of the electronic and optoelectronics properties of new materials based on thienopyrazine for application in dye solar cells. *Journal of Materials and Environmental Science*, 7(3), 700–712.
33. Sang-aroon, W., Laopha, S., Chaiamornnugool, P., Tontapha, S., Saekow, S. et al. (2013). DFT and TDDFT study on the electronic structure and photoelectrochemical properties of dyes derived from cochineal and lac insects as photosensitizer for dye-sensitized solar cells. *Journal of Molecular Modeling*, 19(3), 1407–1415. DOI 10.1007/s00894-012-1692-9.
34. Cherifi, K., Cheknane, A., Hilal, H. S., Benghia, A., Rahmoun, K. et al. (2020). Investigation of triphenylamine-based sensitizer characteristics and adsorption behavior onto ZnTiO₃ perovskite (1 0 1) surfaces for dye-sensitized solar cells using first-principle calculation. *Chemical Physics*, 530, 110595. DOI 10.1016/j.chemphys.2019.110595.
35. Novir, S. B., Hashemianzadeh, S. M. (2015). Density functional theory study of new azo dyes with different π -spacers for dye-sensitized solar cells. *Spectrochimica Acta Part A: Molecular and Biomolecular Spectroscopy*, 143, 20–34. DOI 10.1016/j.saa.2015.02.026.
36. Daoud, A., Cheknane, A., Hilal, H. S., Meftah, A., Benghia, A. (2021). Simulation of electronic and optical properties of polyene-diphenylaniline-sensitizers for perovskite n-ZnTiO₃ towards efficient dye sensitized solar cells. *Materials Science in Semiconductor Processing*, 134, 106037. DOI 10.1016/j.mssp.2021.106037.
37. Daoud, A., Cheknane, A., Touzani, R., Hilal, H. S., Boulouiz, A. (2021). Simulation of the electrochemical properties of dye-sensitized solar cells based on quinoxaline dyes: Effects of hydroxyl group numbers and positions. *Journal of Electronic Materials*, 50(10), 5656–5663. DOI 10.1007/s11664-021-09113-1.
38. Gu, P., Yang, D., Zhu, X., Sun, H., Wangyang, P. et al. (2017). Influence of electrolyte proportion on the performance of dye-sensitized solar cells. *AIP Advances*, 7(10), 105219. DOI 10.1063/1.5000564.